

This is an Open Access document downloaded from ORCA, Cardiff University's institutional repository: <https://orca.cardiff.ac.uk/id/eprint/115676/>

This is the author's version of a work that was submitted to / accepted for publication.

Citation for final published version:

Ruiz De Diego, Irene, Fasano, Stefania , Solis, Oscar, Garcia-Montes, Jose-Ruben, Brea, Jose, Loza, Maria, Brambilla, Riccardo and Rosario, Moratalla 2018. Genetic enhancement of Ras-ERK pathway does not aggravate L-DOPA-induced dyskinesia in mice but prevents the decrease induced by lovastatin. *Scientific Reports* 8 , 15381. 10.1038/s41598-018-33713-3

Publishers page: <https://dx.doi.org/10.1038/s41598-018-33713-3>

Please note:

Changes made as a result of publishing processes such as copy-editing, formatting and page numbers may not be reflected in this version. For the definitive version of this publication, please refer to the published source. You are advised to consult the publisher's version if you wish to cite this paper.

This version is being made available in accordance with publisher policies. See <http://orca.cf.ac.uk/policies.html> for usage policies. Copyright and moral rights for publications made available in ORCA are retained by the copyright holders.



SCIENTIFIC REPORTS



OPEN

Genetic enhancement of Ras-ERK pathway does not aggravate L-DOPA-induced dyskinesia in mice but prevents the decrease induced by lovastatin

Irene Ruiz-DeDiego^{1,2}, Stefania Fasano³, Oscar Solís^{1,2}, José-Rubén García-Montes^{1,2}, José Brea^{4,5}, María I. Loza^{4,5}, Riccardo Brambilla³ & Rosario Moratalla^{1,2}

Increasing evidence supports a close relationship between Ras-ERK1/2 activation in the striatum and L-DOPA-induced dyskinesia (LID). ERK1/2 activation by L-DOPA takes place through the crosstalk between D1R/AC/PKA/DARPP-32 pathway and NMDA/Ras pathway. Compelling genetic and pharmacological evidence indicates that Ras-ERK1/2 inhibition prevents LID onset and may even revert already established dyskinetic symptoms. However, it is currently unclear whether exacerbation of Ras-ERK1/2 activity in the striatum may further aggravate dyskinesia in experimental animal models. Here we took advantage of two genetic models in which Ras-ERK1/2 signaling is hyperactivated, the *Nf1*^{+/-} mice, in which the Ras inhibitor neurofibromin is reduced, and the Ras-GRF1 overexpressing (Ras-GRF1 OE) transgenic mice in which a specific neuronal activator of Ras is enhanced. *Nf1*^{+/-} and Ras-GRF1 OE mice were unilaterally lesioned with 6-OHDA and treated with an escalating L-DOPA dosing regimen. In addition, a subset of *Nf1*^{+/-} hemi-parkinsonian animals was also co-treated with the Ras inhibitor lovastatin. Our results revealed that *Nf1*^{+/-} and Ras-GRF1 OE mice displayed similar dyskinetic symptoms to their wild-type counterparts. This observation was confirmed by the lack of differences between mutant and wild-type mice in striatal molecular changes associated to LID (i.e., FosB, and pERK1/2 expression). Interestingly, attenuation of Ras activity with lovastatin does not weaken dyskinetic symptoms in *Nf1*^{+/-} mice. Altogether, these data suggest that ERK1/2-signaling activation in dyskinetic animals is maximal and does not require further genetic enhancement in the upstream Ras pathway. However, our data also demonstrate that such a genetic enhancement may reduce the efficacy of anti-dyskinetic drugs like lovastatin.

Parkinson's disease (PD) is the second most common neurodegenerative disorder after Alzheimer's disease. This progressive, chronic, and age-related pathology is characterized by a dramatic depletion of dopamine in the striatum following loss of dopaminergic neurons in the substantia nigra pars compacta. Despite extensive investigation aimed at finding new therapeutic approaches, the dopamine precursor molecule L-DOPA remains the most effective and widely used non-invasive therapy for PD. However, in the vast majority of patients, chronic treatment and disease progression cause the appearance of abnormal involuntary movements known as dyskinesias. L-DOPA-induced dyskinesia (LID) interferes significantly with normal motor activity and persists unless L-DOPA dosages are reduced below therapeutic levels. Thus, controlling dyskinetic symptoms is one of the major challenges in PD therapy^{1,2}.

¹Instituto Cajal, Consejo Superior de Investigaciones Científicas (CSIC), Madrid, Spain. ²CIBERNED, Instituto de Salud Carlos III, Madrid, Spain. ³Neuroscience and Mental Health Research Institute (NMHRI), Neuroscience Division, School of Biosciences, Cardiff University, Cardiff, United Kingdom. ⁴Instituto de Farmacia Industrial, Fac de Farmacia, Universidad de Santiago de Compostela, Santiago de Compostela, Spain. ⁵Centro de Investigación CIMUS, Universidad de Santiago de Compostela, Santiago de Compostela, Spain. Correspondence and requests for materials should be addressed to R.M. (email: moratalla@cajal.csic.es)

Received: 4 June 2018
Accepted: 3 October 2018
Published online: 18 October 2018

Extensive work indicates that extracellular signal-regulated kinase 1/2 (ERK1/2) activation in the striatum plays a critical role in the emergence of LID^{1–12}. This activation takes place by two interplaying cascades: the D1R/cAMP/PKA/DARPP-32 pathway and the NMDA/Ras pathway. In the dopamine-depleted striatum, L-DOPA leads to D1R activation and stimulation of adenylyl cyclase through G α olf protein¹³, increasing cAMP accumulation and activating PKA, modulating synaptic plasticity^{14,15}. In turn, PKA phosphorylates DARPP-32 at Thr34^{9,16–18}, which in its phosphorylated state acts as a potent inhibitor of protein phosphatase-1 (PP1). The inhibition of PP-1 thereby controls many downstream effectors, including activation of mitogen-activated protein kinase (MEK, which phosphorylates ERK1/2) and inhibition of STEP (which dephosphorylates ERK1/2)¹⁹. Importantly, genetic deletion or pharmacological blockade of D1R prevents the supersensitive ERK1/2 response and LID^{4,20}.

In addition to D1R-pathway, the ERK1/2 cascade can also be activated by the NMDA receptor via Ras^{21,22}. In this pathway, lovastatin, a drug widely used to treat hyperlipidemia and able to reduce Ras activity by inhibiting its isoprenylation, significantly attenuates the phosphorylation of ERK1/2 and the development of LID^{23,24}. In addition, genetic inactivation of the Ras-guanine nucleotide-releasing factor 1 (Ras-GRF1), a neuronal specific activator of Ras, attenuates dyskinesia in mice and non-human primates^{3,5}.

The neurofibromatosis type 1 (*Nf1*) gene codes for neurofibromin, a cytoplasmic protein that functions as a GTPase-activating protein for Ras^{25,26}. Neurofibromin inhibits Ras activity by catalyzing the conversion of Ras from its active GTP-bound (Ras-GTP) to its inactive GDP-bound form^{27,28}. Reduced neurofibromin expression by *Nf1* gene mutations is associated with increased Ras-ERK1/2 activation^{29,30} and, in the brain, with learning and memory deficits^{27,31–33}. Interestingly, pharmacological inhibition of Ras activity with lovastatin ameliorates the observed behavioral abnormalities in mice and humans^{34–36}. In the present work, we investigated the role of ERK1/2 over-activation in LID with two different approaches: a “direct” approach using Ras-GRF1 overexpressing (Ras-GRF1 OE) transgenic mice, and an “indirect” intervention, favoring the maintenance of Ras in its active form by decreasing the neurofibromin levels using *Nf1*^{+/-} transgenic animals.

Results

Basal locomotor activity and motor coordination are normal in *Nf1*^{+/-} mutant mice. In order to rule out any baseline motor impairment in the mutant mice, we carried out spontaneous locomotor activity and rotarod tests prior to the 6-OHDA lesion. Since previous experiments from Fasano and colleagues³⁷ demonstrated that the increase of Ras-GRF1 expression in Ras-GRF1 OE mice does not affect locomotor activity and motor coordination in these animals, we focused on testing these behavioral performances in *Nf1*^{+/-} mice. *Nf1*^{+/-} and wild-type (WT) mice showed similar horizontal and vertical activity, as indicated by the number of beam breaks measured in a multi-cage activity meter system (Fig. 1A,B). Ambulatory activity measured as total distance traveled was also similar in both genotypes (Fig. 1C). Likewise, there were no statistically significant differences between genotypes in motor coordination (Fig. 1D), measured as the latency to fall from the rotarod. These results indicated that alterations in *Nf1* gene expression do not modify spontaneous locomotor activity or motor coordination.

***Nf1*^{+/-} mutant mice show high striatal Ras-GTP levels but reduced cAMP levels.** Next, to confirm that *Nf1*^{+/-} mice showed a higher activation of the Ras-ERK1/2 signaling pathway, we studied striatal Ras-GTP levels in naïve animals. As expected, we found that *Nf1*^{+/-} mice displayed higher levels of Ras-GTP compared to WT mice (Fig. 1E and supplementary Fig. S1). We also examined whether the mutation in neurofibromin could modulate the activity of G α olf protein by testing cAMP levels in the striatum. Interestingly, we found a decrease in cAMP levels in *Nf1*^{+/-} mutant mice relative to WT counterparts (Fig. 1F).

Heterozygous deletion of *Nf1* has no effect on L-DOPA-induced dyskinesia or LID-associated changes in gene expression. To explore the role of *Nf1* in dyskinesia, we studied the development of LID in hemiparkinsonian/6-OHDA-lesioned mice by scoring axial dystonia and forelimb and orofacial dyskinesias in *Nf1*^{+/-} and their WT littermates. Since high L-DOPA doses can mask subtle differences between genotypes, we used an escalating dosing regimen in which L-DOPA was given i.p. daily for 9 days, with the daily dose increasing over the course of treatment (5, 10, and 20 mg/kg i.p., 3 consecutive days at each dose).

Daily scoring of AIMs (abnormal involuntary movements, i.e., axial dystonia, forelimb and orofacial dyskinesia) revealed a gradual development of dyskinesia in both genotypes, with AIMs scores increasing as the L-DOPA dose ascended. Interestingly, heterozygous *Nf1* mutation had no effect on dyskinetic scores at any of the three L-DOPA doses: there were no significant differences in total dyskinetic scores between *Nf1*^{+/-} and WT mice across the 9-day L-DOPA treatment (Fig. 2D). Both transgenic and WT mice showed great lateral deviation, twisted posture, contralateral forelimb dyskinesia, and jaw movements with tongue protrusion, with no statistically significant differences between genotypes for any of the three AIMs subtypes (Fig. 2A,C).

Correlating with these behavioral results, analysis of the dorsolateral striatum showed that L-DOPA-induced expression of FosB and pERK1/2 were similar in both genotypes (Fig. 3A), as well as pACh3 expression (data not shown). The percentage of denervated striatum also demonstrated no different denervation between groups (Fig. 3B,B').

Overexpression of Ras-GRF1 does not affect L-DOPA-induced dyskinesia. We next explored the effects of direct intervention in Ras signaling by using Ras-GRF1 overexpressing (Ras-GRF1 OE) mice^{37,38}. Ras-GRF1 protein levels in these animals are threefold higher than in WT. Importantly, we previously shown that Ras-GRF1 OE mice are more sensitive to cocaine as measured by enhanced ERK1/2 activation in the striatum and increased behavioral responses³⁷. Similarly to *Nf1*^{+/-} mice, Ras-GRF1 OE animals showed dyskinetic symptoms

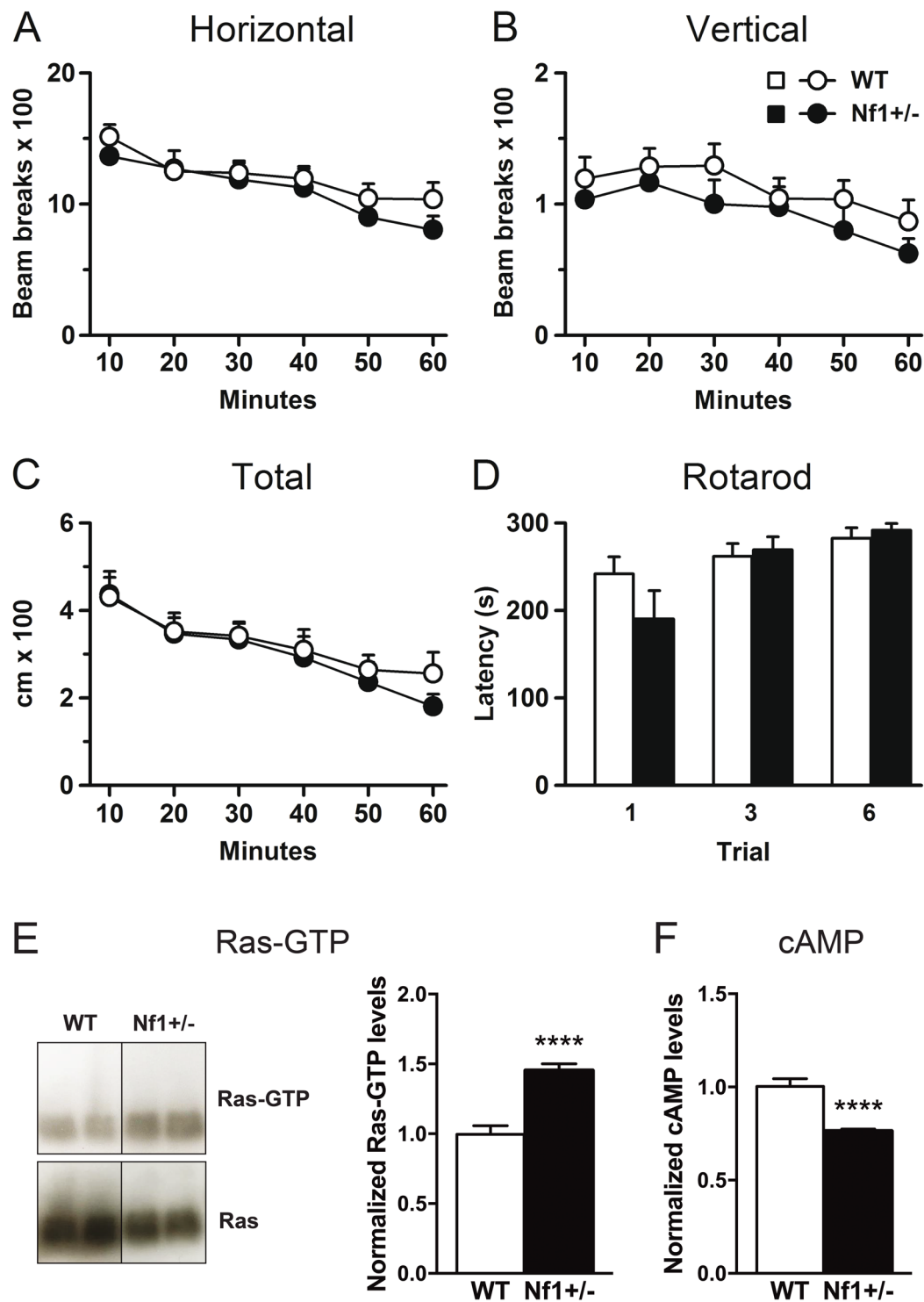


Figure 1. Heterozygous *Nf1* gene mutation does not affect basal locomotor activity but increased striatal Ras-GTP levels. (A) Horizontal and (B) vertical activity and (C) total distance traveled measured for 60 min in a multigage activity meter system. (D) Motor coordination measured in the rotarod at constant acceleration and expressed as latency to fall from the rotating rod. Striatal Ras-GTP levels determined by WB analysis are increased in *Nf1*^{+/-} naïve mice (E) while cAMP levels are decreased compared to their WT counterparts (F). Uncropped blots are provided in Supplementary Fig. S1. *****p* < 0.0001 vs WT. n = 7–12.

upon an escalating dose protocol comparable to WT controls (Fig. 4A). Accordingly, both the percentage of denervated striatum and the striatal expression of pERK1/2 and FosB were indistinguishable between Ras-GRF1 OE and WT mice (Fig. 4B,C).

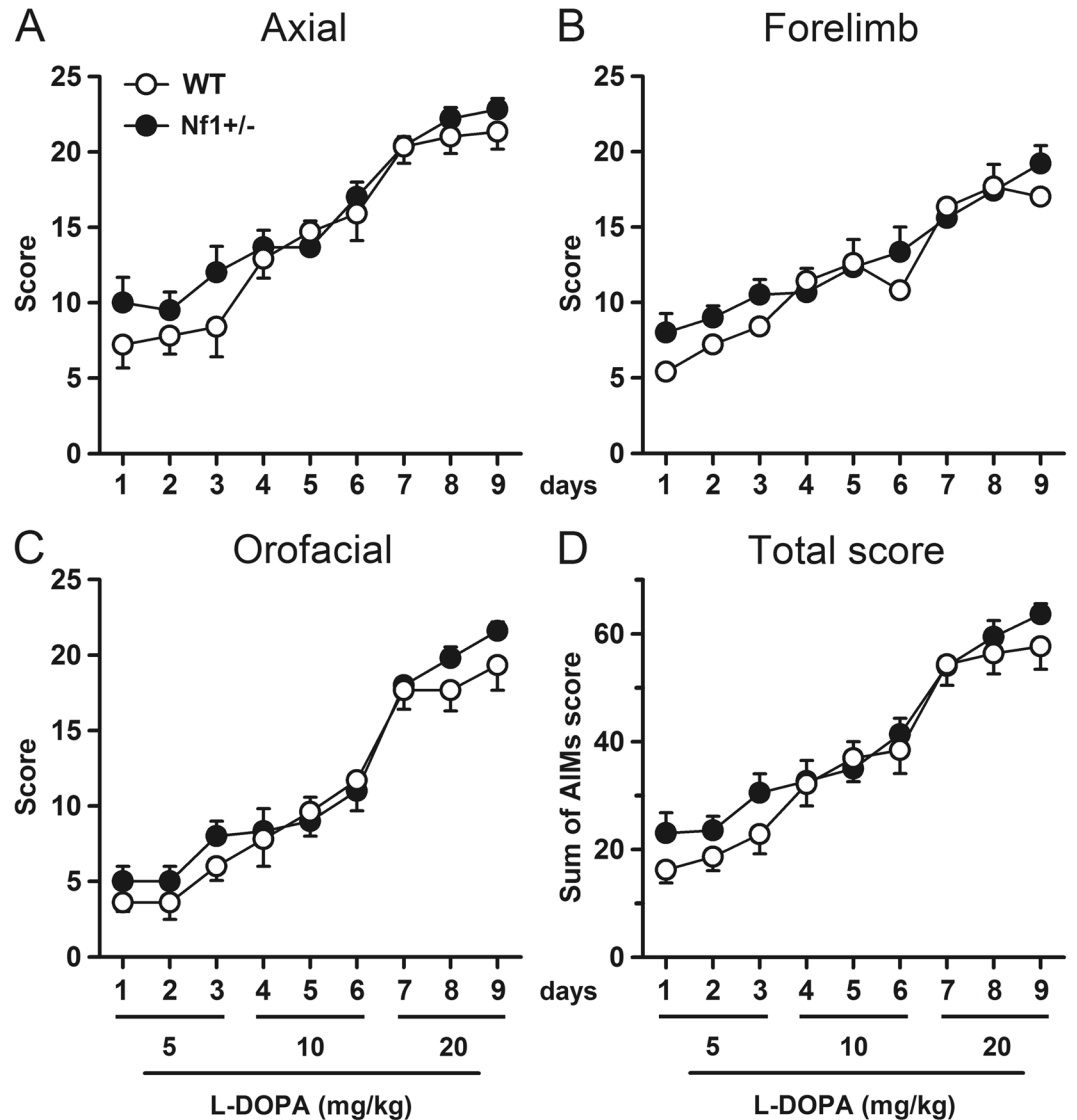


Figure 2. Heterozygous *Nf1* gene mutation does not modify dyskinetic behaviour induced by L-DOPA. Temporal profile of (A) axial dystonia, (B) forelimb dyskinesia, (C) orofacial dyskinesia and (D) cumulated total score induced by an escalating L-DOPA dosing regimen administered in 9 consecutive days. No differences were found between *Nf1*^{+/-} mice and their littermate controls. n = 5–9.

Lovastatin attenuates L-DOPA-induced dyskinesia severity in WT but not in *Nf1*^{+/-} mice. To assess the effect of pharmacological blockade of Ras on LID we used lovastatin, a Ras activity inhibitor. Mice were pretreated with lovastatin (20 mg/kg i.p.) or 0.9% saline for 3 days, as previously described²³. Afterwards, for 10 consecutive days, mice received 20 mg/kg of L-DOPA 2.5 h after lovastatin or saline administration. The time course of AIMS expression following 20 mg/kg L-DOPA treatment was similar in *Nf1*^{+/-} and WT mice (Fig. 5A). Dyskinesia was evident at 20 minutes, peaked between 40 and 60 minutes, declined significantly by 100–120 minutes, and disappeared after 140–160 minutes for both genotypes. WT mice treated with both drugs exhibited significantly less dyskinesia than those treated with L-DOPA only. In contrast, lovastatin had no effect on the intensity of LID in *Nf1*^{+/-} transgenic mice. This difference was reflected in cumulative AIMS scores over the entire 160-min observation period (Fig. 5B). Those scores were reduced by lovastatin in WT mice but not in *Nf1*^{+/-}. Analysis of the individual AIMS over the entire 160-min observation revealed that the effect of lovastatin in WT mice was evident in all the dyskinetic sub-symptoms (Fig. 5C). Intriguingly, lovastatin did not modify frequency or intensity of any individual dyskinetic symptoms in the *Nf1*^{+/-} mutant mice.

To exclude any possible interaction of *Nf1* mutation on the antiparkinsonian properties of L-DOPA, we performed the rotarod test before and after the L-DOPA treatment. In the absence of L-DOPA, parkinsonian animals of both WT and *Nf1*^{+/-} genotypes showed similar latencies to fall from the rotating rod (Fig. 5D), while under chronic L-DOPA treatment both groups of mice showed an improved motor performance, indicating a similar therapeutic response to L-DOPA.

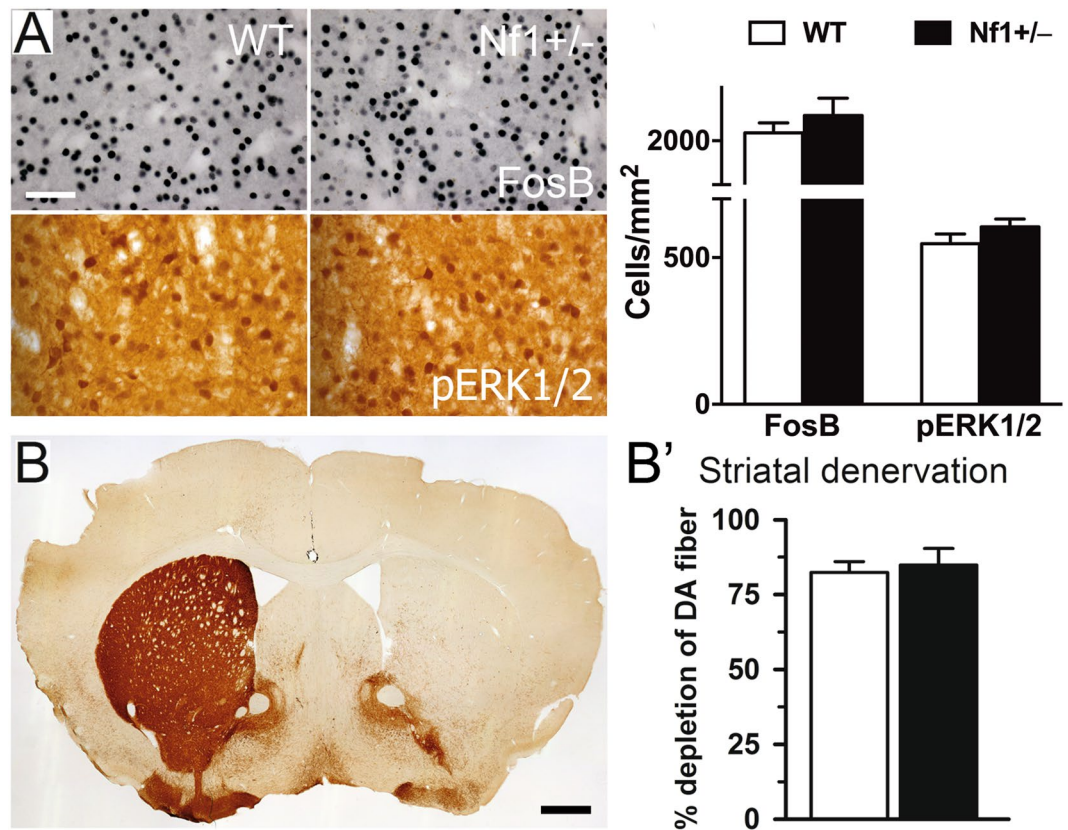


Figure 3. Heterozygous *Nf1* gene mutation does not alter molecular changes induced by L-DOPA. (A) High-power photomicrographs of denervated striatum from WT and heterozygous *Nf1* mice immunostained for FosB and pERK1/2. Histogram represents the quantification of FosB and pERK1/2 immunoreactive positive nuclei. (B) Bar graphs show the percentage of depletion of dopaminergic fibers measured in the striatum. No differences were found between *Nf1*^{+/-} and WT mice. n = 5–9. Scale bars = 50 μ m, 500 μ m.

Discussion

The major finding of this study is that the onset and expression of LID in *Nf1*^{+/-} and in Ras-GRF1 OE mice are indistinguishable from WT. This indicates that a genetic enhancement of the Ras-ERK1/2 pathway does not result in either an exacerbated dyskinetic behavior or in the increase of the associated molecular markers (i.e. FosB, pERK1/2 and pAcH3 expression). Moreover, we demonstrate that pharmacological inhibition of Ras function with lovastatin decreases dyskinetic signs in WT mice, although is unable to reduce LID in the *Nf1*^{+/-} mice.

Since previous works indicate that there is a correlation between Ras-ERK1/2 activity levels and intensity of dyskinetic symptoms^{1,2,6,8,39}, we expected that *Nf1*^{+/-} and Ras-GRF1 OE mice would exhibit more dyskinesia than WT animals. However, this increase in dyskinetic symptoms is not evident in our transgenic mice, nor is an increase in the molecular changes induced by L-DOPA.

As expected, *Nf1*^{+/-} mice showed higher striatal Ras-GTP levels compared to their WT littermates, due to the heterozygous deletion of *Nf1* gene. In heterozygosis, neurofibromin is less efficient at converting Ras-GTP to its inactive form Ras-GDP, leading to higher levels of Ras-GTP as depicted in Fig. 6. On the other hand, this increase in the Ras-ERK1/2 signaling pathway seems to be counterbalanced by a decrease in the G α olf-cAMP pathway, indicated by the lower cAMP striatal levels we found in *Nf1*^{+/-} mice. These results are in line with those found in both *Nf1* patient-derived induced pluripotent stem cell-neural progenitor cells and mouse *Nf1*^{+/-} hippocampal neurons⁴⁰. Thus, we speculate that dyskinetic *Nf1*^{+/-} mice have the Ras-ERK1/2 pathway increased and the G α olf-cAMP pathway decreased in the striatum, generating a net effect similar to that found in WT animals and is responsible for the same dyskinetic behavior displayed. Moreover, a similar scenario could be found in the Ras-GRF1 OE mice since these animals have also increased Ras activity similar to that of the *Nf1*^{+/-} mice. Future experiments to examine striatal cAMP activity in these mice may corroborate this idea.

Despite these negative results, we found that decreasing Ras activity with lovastatin decreases LID in WT mice but not in *Nf1*^{+/-} mice. Chronic co-treatment with lovastatin and L-DOPA effectively decreases dyskinetic symptoms in WT mice, consistent with previous work in hemiparkinsonian rats²³. In our study, we demonstrate that the lovastatin-induced Ras-signaling pathway inhibition significantly reduced all AIMs in WT mice. These results are in line with previous findings using Ras-GRF1 knockout mice⁵, which also showed a decrease in LID. Taken together, this indicates that a direct inhibition in the Ras-ERK1/2 pathway is enough to reduce LID symptoms, but not to abolish them, as occurs when the D1R pathway is altered by a genetic ablation of D1R⁴. NMDA receptor antagonists do not modify ERK1/2 phosphorylation induced by D1R agonists in the denervated

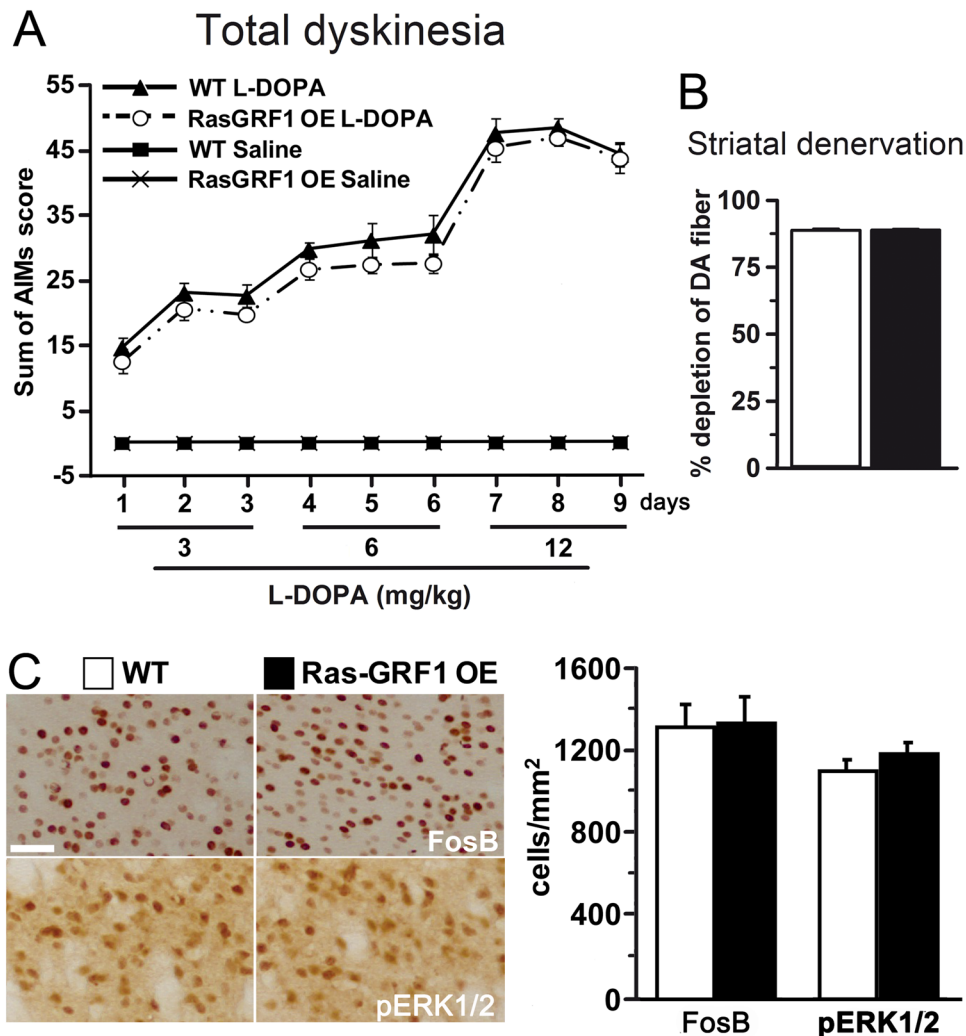


Figure 4. Overexpression of Ras-GRF1 does not alter dyskinetic symptoms or the associated molecular markers induced by L-DOPA. **(A)** Temporal profile of axial, limb and orofacial AIMs induced by an escalating L-DOPA dosing regimen administered in 9 consecutive days. **(B)** Histograms show the percentage of striatal TH immunoreactive fibers depletion as a measure of dopaminergic denervation. **(C)** High-power photomicrographs of striatum from WT and Ras-GRF1 OE mice immunostained for FosB and pERK1/2. Bar graphs represent the quantification of FosB and pERK1/2 immunoreactive positive nuclei. No differences were found between transgenic Ras-GRF1 OE mice and their littermate controls. $n = 10-12$. Scale bar = 50 μm .

striatum⁴¹. Thus, these data suggest that D1R plays a more important role than the NMDA receptor in the control of ERK cascade following chronic L-DOPA treatment. However, it is also important to consider that metabotropic glutamate receptor type 5 (mGluR5) modulates D1R signaling pathway via ERK1/2 activation in the denervated striatum⁴²⁻⁴⁴. For instance, local infusion of a mGluR5 antagonist into the denervated striatum in hemiparkinsonian rats reduced D1R-agonist induced ERK1/2 signaling⁴².

In contrast with that found in WT animals, chronic administration of lovastatin did not diminish LID in transgenic *Nf1*^{+/-} mice, which have upregulated Ras function. Thus, lovastatin Ras-inhibition is not sufficient to reduce dyskinetic symptoms in these mice. These results are in line with previous findings which showed that Ras inhibitors can rescue only some phenotypes in *Nf1*-deficient cell lines⁴⁵ and that lovastatin cannot correct the behavioral or the PET imaging deficits in mice⁴⁶. More recently, Payne and colleagues⁴⁷ performed the last and largest statin study in children with NF1 and concluded that lovastatin is not an effective treatment for cognitive or behavioral deficits in this population. At the signaling level, previous work *in vitro* with hippocampal neurons from *Nf1*^{+/-} mice showed that continuous lovastatin exposure normalizes both the attenuated cAMP levels and increased Ras activity in these mutant cells⁴⁰. Thus, lovastatin decreases LID in WT animals by decreasing Ras activity, while in *Nf1*^{+/-} mice, although it decreases Ras activity, does not change LID, possibly because it may increase cAMP with a null net effect.

Finally, previous experiments demonstrated that the increased Ras-GRF1 expression in Ras-GRF1 OE mice does not affect locomotor activity and motor coordination³⁷. Here we tested these behaviors in *Nf1*^{+/-} mice and found that these animals are indistinguishable from their WT littermates in motor activity and motor coordination, in agreement with previous observations in the open field test³³ and the water maze focusing on swimming

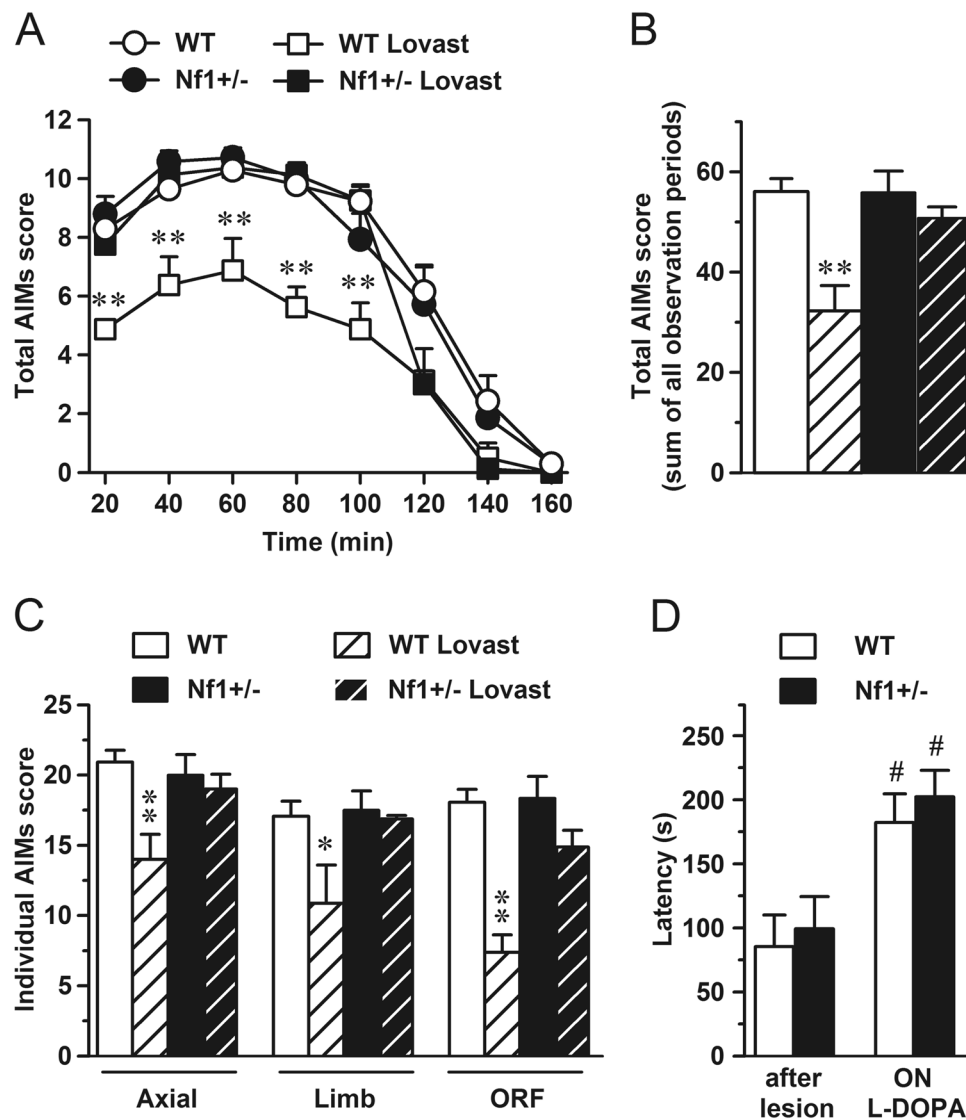


Figure 5. Chronic lovastatin treatment reduces AIMs scores in WT but not in heterozygous *Nf1* mice. **(A)** Time profile of AIMs evaluated for 1 min every 20 min during 160 min on last day of L-DOPA treatment. **(B)** Sum of total AIMs score during all observation periods. **(C)** Sum of all AIM subscores (axial, limb and orofacial) evaluated during all observation periods. **(D)** Motor coordination assessed of hemiparkinsonian mice before L-DOPA treatment (after lesion) and on day 14, 24 h after L-DOPA administration (ON L-DOPA) to verify that genetic manipulation of *Nf1* does not modify the therapeutic effect of L-DOPA. * $p = 0.01$, ** $p < 0.001$ vs WT. # $p < 0.001$ vs after lesion situation. $n = 4-8$.

speed and other motor skills³³ (for review see⁴⁸). Since spontaneous locomotor activity and motor coordination are normal in the *Nf1*^{+/-} mice, results of dyskinesia experiments are not due to motor impairment, but rather to the modification of *Nf1*-related molecular pathways. Importantly, genetic modification in *Nf1*^{+/-} mice does not alter the kinetic profile of L-DOPA, as all animals show similar duration of the L-DOPA response and display similar performance skills in the rotarod test, demonstrating that the antiparkinsonian efficacy of L-DOPA is preserved in all the animals.

In conclusion, it appears from the present study that a plateau in ERK1/2-signaling activation may already be achieved in response to denervation and L-DOPA treatment, therefore a genetic enhancement of the Ras pathway does not exacerbate dyskinetic behavior. However, the lack of anti-dyskinetic effect in response to lovastatin observed in mice with abnormally high Ras activity may be of clinical significance since patients affected by such condition – RASopathies – do exist and may be tested in this respect in the near future.

Methods and Materials

Animals. Since the *Nf1* null mouse is lethal^{35,49}, we used heterozygous mice for the *Nf1* gene (*Nf1*^{+/-})²⁷ obtained by heterozygous mating and genotyped by PCR. Their WT littermates were used as controls. These *Nf1*^{+/-} mutant mice do not develop any abnormalities and are commonly used to study the role of neurofibromin. Ras-guanine nucleotide-releasing factor 1 overexpressing (Ras-GRF1 OE) mice, which exhibit a significant

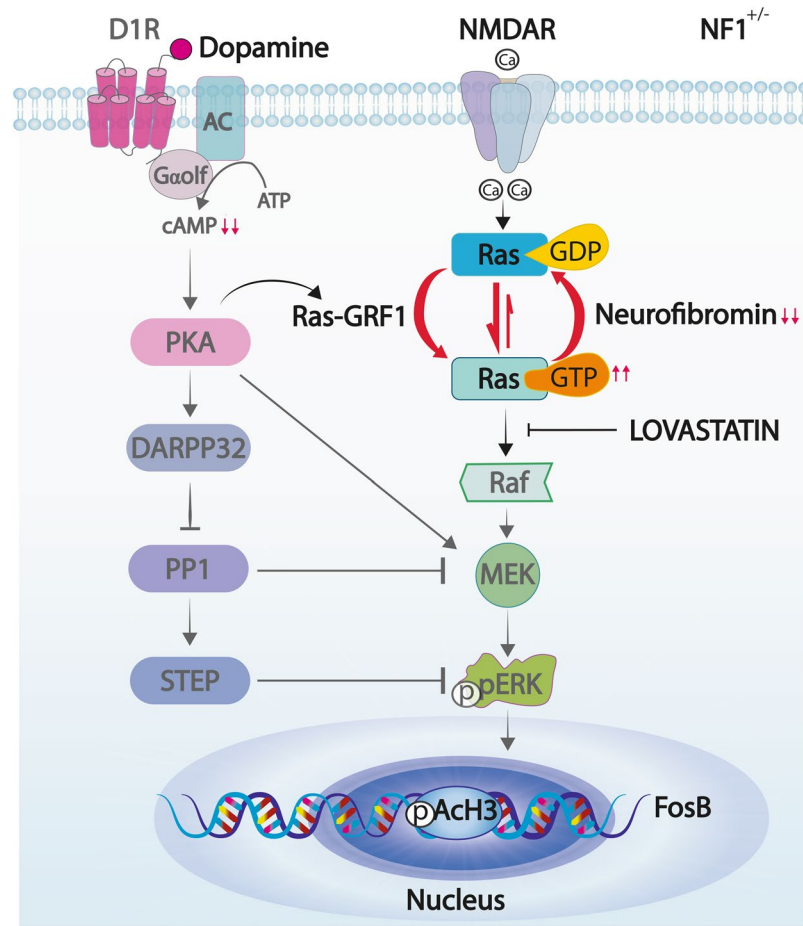


Figure 6. Schematic diagram illustrating D1R and NMDAR signaling cascades in heterozygous *Nf1* mice. In the striatum, dopamine activates D1R leading to cAMP formation and PKA activation that in turn leads to ERK1/2 phosphorylation. In addition, stimulation of NMDAR promotes Ras activation through Ras-GRF1 which catalyzes the conversion of inactive Ras-GDP to active Ras-GTP. This process is counteracted by neurofibromin, which diminishes Ras activity. However, in heterozygosis (*Nf1*^{+/-}) the balance between Ras-GTP and Ras-GDP is displaced towards the active form, favoring ERK1/2 phosphorylation while cAMP levels are reduced.

increase in p140^{Ras-GRF1} protein (three folds to WT levels), were obtained as previously reported^{37,38}. Mice were housed under a 12-h light/dark cycle with *ad libitum* access to food. All experiments were performed in male and female 3–6 month old mice. Experimental protocols were approved by the Cajal Institute Committee on Human and Animal Experimentation and CSIC Ethics Committee, and were in accordance with guidelines of the European Union Council Directive (86/609/European Economic Community).

6-OHDA lesion and drug treatment. *Nf1*^{+/-} mice and their WT littermates were anesthetized with 2% v/v isoflurane and received unilateral stereotaxic injections ($2 \times 2 \mu\text{l}$) of 6-OHDA-HBr (5 $\mu\text{g}/\mu\text{l}$, 20 mM, containing 0.02% ascorbic acid, Sigma-Aldrich, St. Louis, Missouri, USA) in the left striatum at the following coordinates (mm from bregma): AP = +0.65, L = -2 and V = -4 and -3.5, as previously described^{8,50}. Ras-GRF1 OE mice and their WT littermates were lesioned by the administration of 1 μl of 6-OHDA-HBr in the right ascending medial forebrain bundle at the following coordinates: AP = -0.7, L = -1.2 and V = -4.7, as described⁵.

Establishment of L-DOPA-induced dyskinesia: escalating L-DOPA dosing regimen. After 3 weeks of recovery, a set of *Nf1*^{+/-} and WT animals were treated daily for 9 consecutive days with benserazide hydrochloride (10 mg/kg i.p., Sigma-Aldrich), followed 20 minutes later by administration of L-DOPA methyl ester (Sigma-Aldrich), using an escalating dosing regimen with each dose administered for 3 consecutive days (5, 10 and 20 mg/kg i.p.). Similarly, Ras-GRF1 OE mice and their WT littermates were treated for 9 consecutive days with an escalating L-DOPA dosing regimen (3, 6 and 12 mg/kg i.p.) plus benserazide. In all cases control animals were treated daily with saline.

A second group of hemiparkinsonian *Nf1*^{+/-} mice was used to assess the effect of lovastatin on development of LID. Lovastatin (Mevinolin; Sigma-Aldrich), in the lactone form, was dissolved in ethanol and incubated at 50 °C in 0.1 N NaOH for 2 hours for the conversion to the sodium salt. Volume was adjusted with water and pH

was adjusted to 7.5 with HCl^{23,51}. 3-weeks after lesion, mice were pretreated with lovastatin (20 mg/kg i.p.) or 0.9% saline for 3 days. Afterwards, for 10 consecutive days, mice received 20 mg/kg of L-DOPA 2.5 h after lovastatin or saline administration.

Behavioral analysis. *Locomotor activity and motor coordination.* Horizontal and vertical activities, as well as total distance traveled, were recorded in mice as described⁵². Motor coordination was measured using the rotarod (Ugo Basile, Italy) following an accelerating protocol, with increasing speed from 4 to 40 rpm over a 5 minute period as described⁵³. Briefly, mice were tested in 6 consecutive trials 20 minutes apart. Motor coordination was tested before 6-OHDA lesion (naïve), 3 weeks after lesion (Parkinsonian state), and during L-DOPA treatment (dyskinetic state, ON L-DOPA) on day 14, 24 hours after the last L-DOPA injection to avoid overtraining and the peak dyskinesia^{50,54}.

Dyskinetic score. L-DOPA-induced dyskinesia was evaluated using a 0–4 severity scale previously established^{5,8,55,56}. Mice were placed in separate glass cylinders and AIMs were assessed daily for 1 minute (monitoring period) every 20 minutes after L-DOPA over a period of 2 h, or on day 13 in the lovastatin experiment. The total AIMs score is the sum of individual scores for each AIM subtype.

Immunohistochemistry and image analysis. Animals were sacrificed 1 hour after the last L-DOPA injection and perfused and fixed with 4% paraformaldehyde. Brains were cut into 30- μ m-thick coronal sections and immunohistochemistry studies were carried out according to published procedures^{57–59} with the following antibodies: anti-tyrosine-hydroxylase (TH) (1:1000, Millipore, Temecula, CA, USA, ref. AB152), FosB (1:7500, Santa Cruz Biotechnology, Santa Cruz, CA, USA, ref. sc-48), pERK1/2 (1:250; Cell Signaling Technology, ref. 9101 L) and phospho-(Ser10)-acetyl-(Lys14)-histone-3 (pAcH3, 1:1500, Upstate, Cell Signaling Solutions, Lake Placid, NY, USA, ref. 07–081).

Quantification of FosB, pAcH3 and pERK1/2 immunoreactivity was carried out by nucleus count with the “cell counter” plug-in in NIH ImageJ software^{3,5,11}. The number of immunolabelled nuclei was determined in 5–9 animals per group, using 5 serial rostrocaudal sections per animal and 2 counting frames on the dorsolateral striatum per section (0.091 mm² each frame). Images were digitized with a light microscope (Leica, Heidelberg, Germany) under 40x objective. Before counting, images were threshold at a standardized gray-scale level, empirically determined by 2 different observers to allow detection of stained nuclei from low to high intensity, with suppression of very lightly stained nuclei. The data are presented as number of stained nuclei per mm² (mean \pm SEM).

Quantification of TH immunoreactivity fibers in the striatum was performed with the NIH ImageJ software as previously described^{13,60}, analyzing 6–9 rostrocaudal striatal sections per animal. Briefly, 4x lens color images were converted into a gray scale and the area of staining (i.e., denervated area) was quantified as percentage of the total striatal area. Data are presented as the percentage of depletion of dopaminergic fibers.

cAMP and Ras-GTP assay. All assays were performed on dissected striatum, snap-frozen in liquid nitrogen. cAMP levels were quantitated from tissue homogenized in 0.1 M HCl, using a cAMP HTRF kit (CisBio) following manufacturer’s instructions.

Active Ras (Ras-GTP) was detected by Raf1-RBD immunoprecipitation using the RAS activation kit (Millipore). Briefly 500 μ l of homogenized extract were incubated with Raf-1 RBD and agarose for 45 min at 4 °C. Then samples were centrifuged for 10 seconds at 14000 \times g and agarose pellets were washed three times in the same conditions. Pellets were resuspended in 40 μ l of 2X Laemli buffer supplemented with 2 mM DTT and boiled for 5 min at 100 °C. Samples were then processed for WB by following manufacturer’s instructions. Total Ras was also detected as loading control. Both cAMP and Ras-GTP levels were normalized to the levels observed in the striatum of the WT group.

Statistical analysis. Both the behavioral and immunolabeling quantification data of L-DOPA ascending-dose experiment were analyzed by one-way ANOVA. cAMP and Ras-GTP levels data were evaluated by unpaired t-test. Lovastatin experiment data were analyzed by two-way ANOVA followed by Student-Newman-Keuls post hoc test. Differences were considered statistically significant at $p < 0.05$.

Data Availability

The data that support the findings of this study are available from the corresponding author upon reasonable request.

References

1. Bastide, M. F. *et al.* Pathophysiology of L-dopa-induced motor and non-motor complications in Parkinson's disease. *Prog. Neurobiol.* **132**, 96–168 (2015).
2. Murer, M. G. & Moratalla, R. Striatal Signaling in L-DOPA-Induced Dyskinesia: Common Mechanisms with Drug Abuse and Long Term Memory Involving D1 Dopamine Receptor Stimulation. *Front. Neuroanat.* **5**, 51 (2011).
3. Bido, S. *et al.* Differential involvement of Ras-GRF1 and Ras-GRF2 in L-DOPA-induced dyskinesia. *Ann. Clin. Transl. Neurol.* **2**, 662–678 (2015).
4. Darmopil, S., Martin, A. B., De Diego, I. R., Ares, S. & Moratalla, R. Genetic inactivation of dopamine D1 but not D2 receptors inhibits L-DOPA-induced dyskinesia and histone activation. *Biol. Psychiatry* **66**, 603–613 (2009).
5. Fasano, S. *et al.* Inhibition of Ras-guanine nucleotide-releasing factor 1 (Ras-GRF1) signaling in the striatum reverts motor symptoms associated with L-dopa-induced dyskinesia. *Proc. Natl. Acad. Sci. USA* **107**, 21824–21829 (2010).
6. Fasano, S. & Brambilla, R. Ras-ERK Signaling in Behavior: Old Questions and New Perspectives. *Front. Behav. Neurosci.* **5**, 79 (2011).

7. Heumann, R. *et al.* Dyskinesia in Parkinson's disease: mechanisms and current non-pharmacological interventions. *J Neurochem.* **130**, 472–89 (2014).
8. Pavón, N., Martín, A. B., Mendiola, A. & Moratalla, R. ERK phosphorylation and FosB expression are associated with L-DOPA-induced dyskinesia in hemiparkinsonian mice. *Biol. Psychiatry* **59**, 64–74 (2006).
9. Santini, E. *et al.* Critical involvement of cAMP/DARPP-32 and extracellular signal-regulated protein kinase signaling in L-DOPA-induced dyskinesia. *J. Neurosci.* **27**, 6995–7005 (2007).
10. Solís, O., Espadas, I., Del-Bel, E. A. & Moratalla, R. Nitric oxide synthase inhibition decreases L-DOPA-induced dyskinesia and the expression of striatal molecular markers in Pitx3(−/−) aphakia mice. *Neurobiol. Dis.* **73**, 49–59 (2015).
11. Solís, O., García-Montes, J. R., González-Granillo, A., Xu, M. & Moratalla, R. Dopamine D3 Receptor Modulates L-DOPA-Induced Dyskinesia by Targeting D1 Receptor-Mediated Striatal Signaling. *Cereb. Cortex* **27**, 435–446 (2017).
12. Westin, J. E., Vercammen, L., Strome, E. M., Konradi, C. & Cenci, M. A. Spatiotemporal pattern of striatal ERK1/2 phosphorylation in a rat model of L-DOPA-induced dyskinesia and the role of dopamine D1 receptors. *Biol. Psychiatry* **62**, 800–810 (2007).
13. Ruiz-DeDiego, I., Naranjo, J. R., Hervé, D. & Moratalla, R. Dopaminergic regulation of olfactory type G-protein alpha subunit expression in the striatum. *Mov. Disord.* **30**, 1039–1049 (2015).
14. Suarez, L. M., Solís, O., Aguado, C., Lujan, R. & Moratalla, R. L-DOPA Oppositely Regulates Synaptic Strength and Spine Morphology in D1 and D2 Striatal Projection Neurons in Dyskinesia. *Cereb. Cortex* **26**, 4253–4264 (2016).
15. Suarez, L. M., Alberquilla, S., García-Montes, J. R. & Moratalla, R. Differential Synaptic Remodeling by Dopamine in Direct and Indirect Striatal Projection Neurons in Pitx3−/− Mice, a Genetic Model of Parkinson's Disease. *J Neurosci* **38**, 3619–3630 (2018).
16. Bateup, H. S. *et al.* Distinct subclasses of medium spiny neurons differentially regulate striatal motor behaviors. *Proc. Natl. Acad. Sci. USA* **107**, 14845–14850 (2010).
17. Picconi, B. *et al.* Loss of bidirectional striatal synaptic plasticity in L-DOPA-induced dyskinesia. *Nat. Neurosci.* **6**, 501–506 (2003).
18. Santini, E. *et al.* Distinct changes in cAMP and extracellular signal-regulated protein kinase signalling in L-DOPA-induced dyskinesia. *PLoS One* **5**, e12322 (2010).
19. Valjent, E. *et al.* Regulation of a protein phosphatase cascade allows convergent dopamine and glutamate signals to activate ERK in the striatum. *Proc. Natl. Acad. Sci. USA* **102**, 491–496 (2005).
20. Santini, E. *et al.* L-DOPA activates ERK signaling and phosphorylates histone H3 in the striatonigral medium spiny neurons of hemiparkinsonian mice. *J. Neurochem.* **108**, 621–633 (2009).
21. Hayashi, T. & Huganir, R. L. Tyrosine phosphorylation and regulation of the AMPA receptor by SRC family tyrosine kinases. *J. Neurosci.* **24**, 6152–6160 (2004).
22. Ivanov, A. *et al.* Opposing role of synaptic and extrasynaptic NMDA receptors in regulation of the extracellular signal-regulated kinases (ERK) activity in cultured rat hippocampal neurons. *J. Physiol.* **572**, 789–798 (2006).
23. Schuster, S. *et al.* The 3-hydroxy-3-methylglutaryl-CoA reductase inhibitor lovastatin reduces severity of L-DOPA-induced abnormal involuntary movements in experimental Parkinson's disease. *J. Neurosci.* **28**, 4311–4316 (2008).
24. Tison, F. *et al.* Simvastatin decreases levodopa-induced dyskinesia in monkeys, but not in a randomized, placebo-controlled, multiple cross-over (“n-of-1”) exploratory trial of simvastatin against levodopa-induced dyskinesia in Parkinson's disease patients. *Parkinsonism Relat Disord.* **19**, 416–21 (2013).
25. Ballester, R. *et al.* The NF1 locus encodes a protein functionally related to mammalian GAP and yeast IRA proteins. *Cell* **63**, 851–859 (1990).
26. Xu, G. F. *et al.* The catalytic domain of the neurofibromatosis type 1 gene product stimulates ras GTPase and complements ira mutants of *S. cerevisiae*. *Cell* **63**, 835–841 (1990).
27. Costa, R. M. *et al.* Mechanism for the learning deficits in a mouse model of neurofibromatosis type 1. *Nature* **415**, 526–530 (2002).
28. Jacks, T. *et al.* Tumour predisposition in mice heterozygous for a targeted mutation in Nf1. *Nat. Genet.* **7**, 353–361 (1994).
29. Basu, T. N. *et al.* Aberrant regulation of ras proteins in malignant tumour cells from type 1 neurofibromatosis patients. *Nature* **356**, 713–715 (1992).
30. DeClue, J. E., Cohen, B. D. & Lowy, D. R. Identification and characterization of the neurofibromatosis type 1 protein product. *Proc. Natl. Acad. Sci. USA* **88**, 9914–9918 (1991).
31. Costa, R. M. & Silva, A. J. Mouse models of neurofibromatosis type I: bridging the GAP. *Trends Mol. Med.* **9**, 19–23 (2003).
32. Cui, Y. *et al.* Neurofibromin regulation of ERK signaling modulates GABA release and learning. *Cell.* **135**, 549–560 (2008).
33. Silva, A. J. *et al.* A mouse model for the learning and memory deficits associated with neurofibromatosis type I. *Nat. Genet.* **15**, 281–284 (1997).
34. Bearden, C. E. *et al.* A randomized placebo-controlled lovastatin trial for neurobehavioral function in neurofibromatosis I. *Ann Clin Transl Neurol.* **3**, 266–79 (2013).
35. Li, W. *et al.* The HMG-CoA reductase inhibitor lovastatin reverses the learning and attention deficits in a mouse model of neurofibromatosis type 1. *Curr. Biol.* **15**, 1961–1967 (2005).
36. Mainberger, F. *et al.* Lovastatin improves impaired synaptic plasticity and phasic alertness in patients with neurofibromatosis type 1. *BMC Neurol.* **13**, 131 (2013).
37. Fasano, S. *et al.* Ras-guanine nucleotide-releasing factor 1 (Ras-GRF1) controls activation of extracellular signal-regulated kinase (ERK) signaling in the striatum and long-term behavioral responses to cocaine. *Biol. Psychiatry* **66**, 758–768 (2009).
38. Yoon, B. *et al.* Rasgrf1 imprinting is regulated by a CTCF-dependent methylation-sensitive enhancer blocker. *Mol. Cell Biol.* **25**, 11184–11190 (2005).
39. Feyder, M., Bonito-Oliva, A. & Fisone, G. L-DOPA-Induced Dyskinesia and Abnormal Signaling in Striatal Medium Spiny Neurons: Focus on Dopamine D1 Receptor-Mediated Transmission. *Front. Behav. Neurosci.* **5**, 71 (2011).
40. Anastasaki, C. & Gutmann, D. H. Neuronal NF1/RAS regulation of cyclic AMP requires atypical PKC activation. *Hum. Mol. Genet.* **23**, 6712–6721 (2014).
41. Gerfen, C. R., Miyachi, S., Paletzki, R. & Brown, P. D1 dopamine receptor supersensitivity in the dopamine-depleted striatum results from a switch in the regulation of ERK1/2/MAP kinase. *J Neurosci* **22**, 5042–54 (2002).
42. Fieblinger, T. Mechanisms of dopamine D1 receptor-mediated ERK1/2 activation in the parkinsonian striatum and their modulation by metabotropic glutamate receptor type 5. *J Neurosci.* **34**, 4728–40 (2014).
43. Rylander, D. *et al.* Pharmacological modulation of glutamate transmission in a rat model of L-DOPA-induced dyskinesia: effects on motor behavior and striatal nuclear signaling. *J Pharmacol Exp Ther.* **330**, 227–35 (2009).
44. Sebastianutto, I. & Cenci, M. A. mGlu receptors in the treatment of Parkinson's disease and L-DOPA-induced dyskinesia. *Curr Opin Pharmacol.* **38**, 81–89 (2018).
45. Kim, H. A., Ling, B. & Ratner, N. Nf1-deficient mouse Schwann cells are angiogenic and invasive and can be induced to hyperproliferate: reversion of some phenotypes by an inhibitor of farnesyl protein transferase. *Mol. Cell Biol.* **17**, 862–872 (1997).
46. Brown, J. A. *et al.* PET imaging for attention deficit preclinical drug testing in neurofibromatosis-1 mice. *Exp. Neurol.* **232**, 333–8 (2011).
47. Payne, J. M. *et al.* Randomized placebo-controlled study of lovastatin in children with neurofibromatosis type 1. *Neurology.* **87**, 2575–2584 (2016).
48. Shilyansky, C., Lee, Y. S. & Silva, A. J. Molecular and cellular mechanisms of learning disabilities: a focus on NF1. *Annu. Rev. Neurosci.* **33**, 221–243 (2010).

49. Brannan, C. I. *et al.* Targeted disruption of the neurofibromatosis type-1 gene leads to developmental abnormalities in heart and various neural crest-derived tissues. *Genes Dev.* **8**, 1019–1029 (1994).
50. Ruiz-DeDiego, I., Mellstrom, B., Vallejo, M., Naranjo, J. R. & Moratalla, R. Activation of DREAM (Downstream Regulatory Element Antagonistic Modulator), a calcium-binding protein, reduces L-DOPA-induced dyskinesias in mice. *Biol. Psychiatry* **77**, 95–105 (2015).
51. Kita, T., Brown, M. S. & Goldstein, J. L. Feedback regulation of 3-hydroxy-3-methylglutaryl coenzyme A reductase in livers of mice treated with mevlinolin, a competitive inhibitor of the reductase. *J. Clin. Invest.* **66**, 1094–1100 (1980).
52. Granado, N. *et al.* D1 but not D5 dopamine receptors are critical for LTP, spatial learning, and LTP-Induced arc and zif3268 expression in the hippocampus. *Cereb. Cortex* **18**, 1–12 (2008).
53. Gonzalez-Aparicio, R. & Moratalla, R. Oleoylethanolamide reduces L-DOPA-induced dyskinesia via TRPV1 receptor in a mouse model of Parkinson's disease. *Neurobiol. Dis.* **62**, 416–425 (2014).
54. Espadas, I. *et al.* L-DOPA-induced increase in TH-immunoreactive striatal neurons in parkinsonian mice: insights into regulation and function. *Neurobiol. Dis.* **48**, 271–281 (2012).
55. Lundblad, M., Picconi, B., Lindgren, H. & Cenci, M. A. A model of L-DOPA-induced dyskinesia in 6-hydroxydopamine lesioned mice: relation to motor and cellular parameters of nigrostriatal function. *Neurobiol. Dis.* **16**, 110–123 (2004).
56. Suárez, L. M. *et al.* L-DOPA Treatment Selectively Restores Spine Density in Dopamine Receptor D2-Expressing Projection Neurons in Dyskinetic Mice. *Biol. Psychiatry* **75**, 711–722 (2014).
57. Ares-Santos, S. *et al.* Dopamine D(1) receptor deletion strongly reduces neurotoxic effects of methamphetamine. *Neurobiol. Dis.* **45**, 810–820 (2012).
58. Ares-Santos, S., Granado, N., Espadas, I., Martinez-Murillo, R. & Moratalla, R. Methamphetamine causes degeneration of dopamine cell bodies and terminals of the nigrostriatal pathway evidenced by silver staining. *Neuropsychopharmacology* **39**, 1066–1080 (2014).
59. Granado, N. *et al.* Selective vulnerability in striosomes and in the nigrostriatal dopaminergic pathway after methamphetamine administration: early loss of TH in striosomes after methamphetamine. *Neurotox Res.* **18**, 48–58 (2008).
60. Mendieta, L., Granado, N., Aguilera, J., Tizabi, Y. & Moratalla, R. Fragment C Domain of Tetanus Toxin Mitigates Methamphetamine Neurotoxicity and Its Motor Consequences in Mice. *Int J Neuropsychopharmacol.* **19**, 1–11 (2016).

Acknowledgements

We would like to thank Mrs. Emilia Rubio, Ms. Beatriz Pro and Mr. Mario Berrocal for their excellent technical assistance.

Author Contributions

I.R.D.D. Performed the experiments, carried out data quantification, prepared the figures and wrote the first draft. S.F. Performed the experiments, carried out data quantification, prepared the figures and reviewed the manuscript. O.S. Performed the experiments, carried out data quantification, prepared the figures and reviewed the manuscript. J.R.G.M. Carried out data quantification, prepared Figure 6 and reviewed the manuscript. J.M.B. cAMP and Ras-GTP assays and data analysis and quantification. M.I.L. cAMP and Ras-GTP assays and data analysis and quantification. R.B. Provided the experimental design, data analysis, procured funding, and interpretation of the results and reviewed the manuscript. R.M. Conceived the study, provided the experimental design, data analysis, procured funding, and interpretation of the results and the final version of the manuscript. This work was supported by grants from the Spanish Ministerios de Economía y Competitividad and of Sanidad Política Social e Igualdad, ISCIII: SAF2016-78207-R, CIBERNED ref. CB06/05/0055, PNSD 2016/33 and PCIN 2015–098 and Foundation Ramon Areces (to RM) and by the Michael J. Fox Foundation for Parkinson's Research, Parkinson's UK, the Italian Ministry of Health and the Compagnia di San Paolo (to RB).

Additional Information

Supplementary information accompanies this paper at <https://doi.org/10.1038/s41598-018-33713-3>.

Competing Interests: The authors declare no competing interests.

Publisher's note: Springer Nature remains neutral with regard to jurisdictional claims in published maps and institutional affiliations.



Open Access This article is licensed under a Creative Commons Attribution 4.0 International License, which permits use, sharing, adaptation, distribution and reproduction in any medium or format, as long as you give appropriate credit to the original author(s) and the source, provide a link to the Creative Commons license, and indicate if changes were made. The images or other third party material in this article are included in the article's Creative Commons license, unless indicated otherwise in a credit line to the material. If material is not included in the article's Creative Commons license and your intended use is not permitted by statutory regulation or exceeds the permitted use, you will need to obtain permission directly from the copyright holder. To view a copy of this license, visit <http://creativecommons.org/licenses/by/4.0/>.

© The Author(s) 2018